



ELSEVIER

Applied Surface Science 183 (2001) 10–17

applied
surface science

www.elsevier.com/locate/apsusc

Laser ablation and deposition of Bioglass[®] 45S5 thin films

L. D'Alessio^a, D. Ferro^b, V. Marotta^c, A. Santagata^a, R. Teghil^{a,*}, M. Zaccagnino^a

^aDipartimento di Chimica, Università della Basilicata, via N. Sauro 85, 85100 Potenza, Italy

^bCNR Centro di Termodinamica Chimica alle Alte Temperature, P.le A. Moro 5, 00185 Roma, Italy

^cCNR Istituto Materiali Speciali, via S. Loja, Tito Scalo (PZ), Italy

Received 22 May 2001; accepted 31 July 2001

Abstract

A study of the laser ablation and deposition, on Ti6Al4V substrates, of a biological active glass (Bioglass[®] 45S5) is reported. The gaseous phase composition has been determined by laser ablation inductively coupled plasma mass spectrometry, optical imaging and emission spectroscopy. The deposited films were studied by scanning electron microscopy coupled with energy and wavelength dispersive X-ray analysis and X-ray diffraction. The adhesion of films to the substrates has been studied by scratch tests. Moreover, after exposing the coatings to a simulating body fluid solution, their bioactivity has been monitored by X-ray diffraction analysis of the hydroxylapatite growth. This procedure has been followed for different time scales up to a maximum of 24 days.

The deposition mechanism seems to be related mainly to the mechanical transport of the target material in form of droplets, while the gaseous phase, having a very different composition, plays a marginal role. The overall film retains the target stoichiometry and bioactivity in a large range of experimental conditions. © 2001 Elsevier Science B.V. All rights reserved.

PACS: 81.15Fg; 81.05 Kf

Keywords: Laser ablation; Thin film deposition; Biomaterials

1. Introduction

The materials commonly used in medicine can be divided as a consequence of their behaviour in the biological environment, in bioinert and bioactive. The former term is used for materials which have high stability and no biological reaction within the human body, while, on the contrary, the latter refers to compounds whose performances are improved by their interaction with the living tissues. In the last years, a wide range of bioactive materials, including

sintered hydroxylapatite, glass ceramics and glasses, have been developed, as coatings on metals and metal alloys, and applied in the field of artificial bones [1,2].

We have focalised our interest on bioactive glasses because these materials appear to be very promising, for their performance in promoting a rapid new bone formation. Traditionally bioactive glasses are deposited by plasma spraying and electrophoretic deposition methods [3–5] even though other useful techniques recently developed may be used. In particular pulsed laser ablation and deposition (PLAD) is nowadays widely used in order to deposit mono- and multi-layer thin films of materials of technological interest. These include high T_c superconductors, semiconductors, ferroelectrics, metals, metal alloys, dielectrics and

* Corresponding author. Tel.: +39-971-202225;

fax: +39-971-202223.

E-mail address: teghil@unibas.it (R. Teghil).

hydroxylapatite [6,7]. Glasses are very interesting materials even because the ablation mechanism, probably led by their defects, is often extremely complex and, therefore, hard to be foreseen.

The material we have used as ablation target was Bioglass[®] 45S5. It is a glass containing silicon, calcium, sodium and phosphorus oxides and its importance is related to its capability, when in contact with body fluids, to stimulate the growth of calcium hydroxylapatite on its surface. Calcium hydroxylapatite is the main mineral component of bone and its growth is due to an ionic exchange mechanism between the glass surface and the body fluids [8]. Bioglass can be used to coat titanium dental screws or other prosthetic objects, that in many cases have the ideal dimension for the use of PLAD as deposition technique.

In a preliminary work [9], we showed that was possible to deposit films with the right stoichiometry by laser ablation of a Bioglass target. In this paper, we will analyse more in detail the ablated gaseous phase and the deposited films in order to clarify the ablation–deposition mechanism and evaluate the real bioactivity of our Bioglass coatings.

2. Experimental

The experimental set up for laser ablation and deposition experiments has been already described [9]. It consists of a vacuum chamber, equipped with a rotating target and a heatable substrate holder. The laser used for the ablation was a doubled Nd:YAG laser ($\lambda = 532$ nm, $\tau = 7$ ns, 10 Hz repetition rate) at fluences between 0.5 and 14 J/cm². The targets were commercial Bioglass[®] 45S5 from US Biomaterials and the deposition substrate (a Ti6Al4V alloy) was in off-axis position. This choice was made for minimising the presence of splinters on the film surface. The background pressure was kept at 10⁻⁴ Pa. The analysis of the gaseous phase was carried out by emission spectroscopy (Optical Multichannel Analyser OMA III EG&G), ICCD imaging (Princeton ICCD camera, 5 ns time resolution) and laser ablation inductively coupled plasma mass spectrometry (LA-ICP-MS). The ICCD camera and the OMA spectrometer were on line. Vice versa the mass spectra were obtained off line by using a Perkin Elmer Elan 5000 coupled with a

laser ablation cell homemade apparatus. In order to perform the LA-ICP-MS calibration, the 1834, 278 and 81_a NIST standards have been exploited. The 1834 sample has been provided in a disk form with diameter of 30 mm. Therefore, it has been analysed directly by LA-ICP-MS. On the contrary, since the other two standards were in the powder form, they have been firstly pressed for 30 min in a circular stainless steel die and 10 tonnes of pressure. In this way 30 mm diameter disks have been obtained even for these samples, which, successively, have been analysed by LA-ICP-MS. The data so obtained, by the LA-ICP-MS analysis of the three standards, have allowed us to define a mean calibration factor for each one of the four elements forming the Bioglass 45S5. Thus, by applying the correction factor previously calculated, it has been possible to define the amount, as weight percentage, of each element detected by LA-ICP-MS analysis of the Bioglass 45S5.

The techniques used to study the deposited films were standard techniques such as X-ray diffraction (Siemens D5000 using Cu K α 1 radiation), scanning electron microscopy (SEM, Cambridge Stereoscan 100, 7 nm resolution) coupled with energy dispersive (EDX) and wavelength dispersive (WDX) X-ray analysis and scratch test (SP-11 Scratch Tester).

3. Results and discussion

The nominal composition of the Bioglass target (at.%) is Na 30.3, Ca 23.2, Si 43.8, P 2.8 [9], excluding the oxygen percentage to allow a direct comparison with EDX results. On the other hand, emission spectra data show a very different composition of the gas phase coming from target ablation. The assignment of the emission spectrum, which has been already reported [9], shows that the emission intensity of Si and P is very low, due probably to their concentration. This is not surprising for phosphorous, present in a small amount also in the target, but indicates that silicon is no more the main constituent of the gas phase of the plume.

In order to confirm the emission data, we have studied the ablation plume by LA-ICP-MS. By using this technique it is possible to obtain quantitative information on the plume composition and in particular on

Table 1
Gas phase composition of the ablated material by LA-ICP-MS analysis

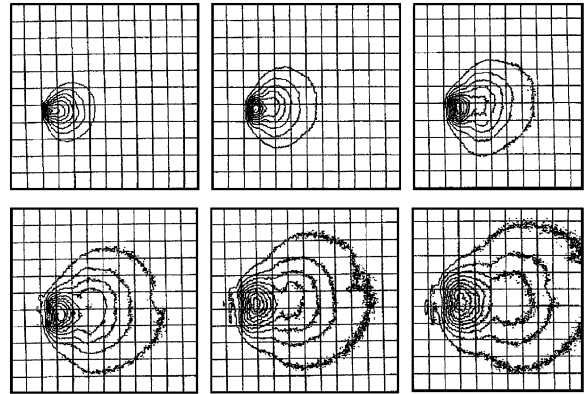
	Na (at.%)	Ca (at.%)	Si (at.%)	P (at.%)
Target	30.2	23.2	43.8	2.8
Gas phase	36.0	44.1	19.5	0.4

its gaseous part, because the particulate is not efficiently transported to the torch and not efficiently ionised [10]. A comparison between ablation target and ablated gas phase composition is reported in Table 1. It is clear that we have a great lack of P and in particular of Si (from about 44 to 20%), demonstrating that under our laser fluence conditions (from 3.5, which is the ablation threshold, up to 15 J/cm²) the ablation can be considered to be not congruent.

In Fig. 1, the contour plots from the ICCD camera images representing the time evolution of the ablated plume are shown (a), together with the values for front velocity and cosine exponent (b). n is the cosine exponent in the equation $I(\theta) = I_0 \cos^n \theta$, where $I(\theta)$ is the flux intensity along a direction forming an angle θ with the normal to the target surface, and I_0 the intensity corresponding to $\theta = 0$. It is a parameter related to the anisotropy of the distribution: in fact $n = 1$ corresponds to a perfectly spherical distribution.

The ICCD data are not particularly useful because the system is too complicate (five elements) to allow, e.g., any interpretation about the presence of two maximums in the plume. In other, more simple systems, such as AlN, the presence of a double maximum is related to the different velocities of the neutral and ionised parts of the plume [11], but it is interesting to note that no particle emission has been revealed by this technique.

We can explain the gas phase characteristics by considering the Bioglass structure [12], where P atoms, occupying some Si sites in the glass network, are strongly oriented and covalently bound to oxygen atoms, as well as Si. On the contrary Na and Ca ions have a high mobility in the glass network, as a consequence of the ionic character of their bonds with oxygen. Consequently, it is easier to remove Ca and Na in comparison with Si and P, especially if the surface temperature is not very high.



(a)

Laser Fluence (J/cm ²)	Front Velocity (10 ⁶ cm/s)	n
4.2	2.2	0.6
7.2	3.9	0.8
8.2	5.7	1.2

(b)

Fig. 1. (a) Intensity contour plots from ICCD camera images showing the temporal evolution of the plume (laser fluence: 4.2 J/cm²). The first image is 100 ns delayed with respect to the laser pulse and the others have been acquired with steps of 100 ns. (b) Plume front velocity and cosine exponent (n) at different laser fluences.

These results should indicate that PLAD is not an useful technique in this case, since the sample vaporisation induced by laser seems to be not congruent. Nonetheless, before taking any conclusion, we should examine the deposited film characteristics.

Informations about the distribution of film thickness on the substrate have been obtained by optical interferometry [13]. Due to the transparency of the Bioglass film, the observation of the sample in reflected light is accompanied by the formation of interference patterns (Newton rings). In Fig. 2a, contrast-enhanced, greyscale image of the film, showing the interference fringes is reported. The dark lines can be considered as contour plot curves and are representative of the slope of the film surface. The

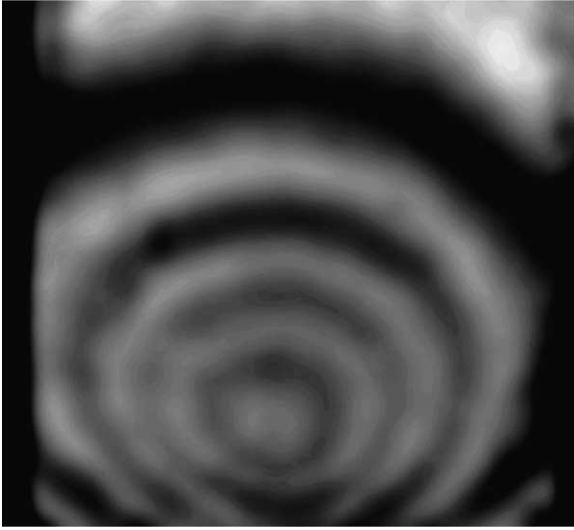


Fig. 2. Interference patterns of a $5 \times 5 \text{ mm}^2$ substrate covered by Bioglass (laser fluence = 7 J/cm^2 , deposition time = $15'$) obtained by a reflectance operating scanner.

distance between two consecutive lines corresponds to a difference of about 275 nm in the film thickness.

Fig. 3 shows the SEM microphotographs of surface and cross-section of a film deposited by Bioglass laser ablation. It is evident that the main constituent of the film is a large number of droplets, embedded in a continuous matrix. As already reported [9] in some cases small needle crystals are present on the film surface. The overall morphology does not change with laser fluence in our experimental range ($0.5\text{--}14 \text{ J/cm}^2$).

The film elemental composition analysed by EDX is reported in Table 2. The droplets composition is close to the target composition, while the matrix shows a lower content of silicon and phosphorous. The needle crystals composition is clearly different from the target one. The analyses on the matrix and on

Table 2
EDX analysis of a Bioglass thin film

	Na (at.%)	Ca (at.%)	Si (at.%)	P (at.%)
Target	30.2	23.2	43.8	2.8
Droplets	32.8	22.7	42.2	2.3
Matrix	34.2	27.3	38.0	0.5
Crystals	45.0	22.0	33.0	0.0
Mean value	33.0	23.1	42.2	1.7

Table 3

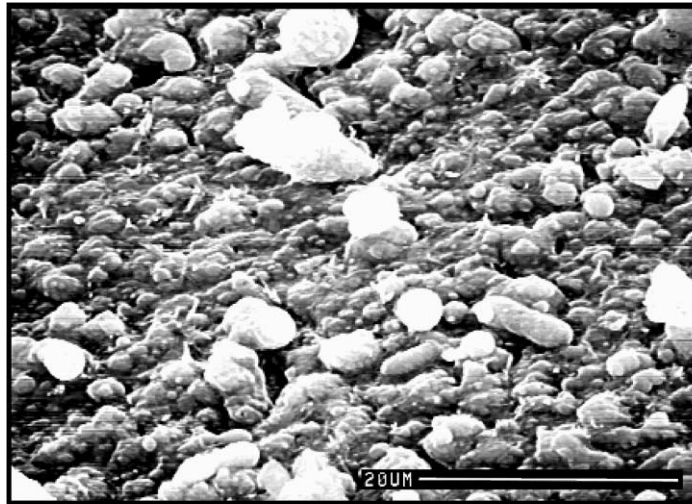
Comparison between EDX and WDX analyses of the same Bioglass film of Table 2

	Na (at.%)	Ca (at.%)	Si (at.%)	P (at.%)
Target	30.2	23.2	43.8	2.8
Mean value (EDX)	33.0	23.1	42.2	1.7
Mean value (WDX)	32.8	24.0	40.4	2.8

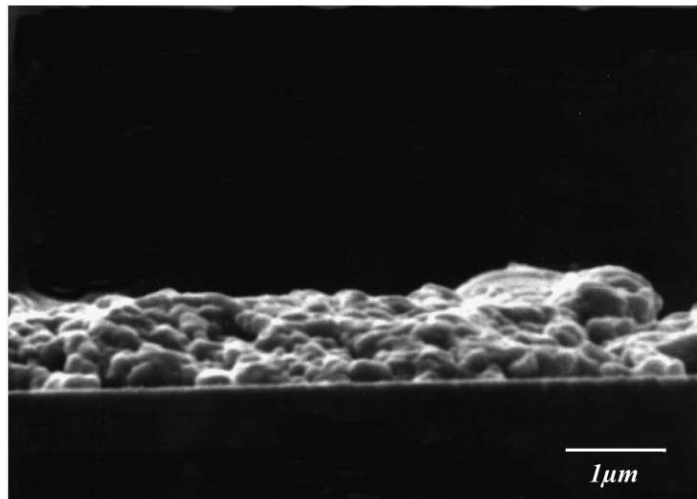
the crystals are not really quantitative and can give only a rough indication about the real composition, because the EDX technique is not a surface technique. Furthermore, when we perform a crystal analysis we cannot avoid the interference of the film lying below it. As a consequence, probably, matrix and crystals real compositions are much different from the target one than what is shown in our analysis. In any case the mean composition, considered as the composition on a large area, is close to the target one and seems to indicate that the droplets are largely the main component of the film.

In order to evaluate the accuracy of our EDX composition data, we compared them with those obtained by using WDX. Table 3 shows all resulting data, and we can notice a good agreement between these two techniques.

The presence of droplets on a film surface is not an unusual feature in PLAD experiments, but the large number of these droplets in our case requires an explanation. A SEM microphotograph of the target surface after laser ablation (Fig. 4a) shows a melted surface with a great number of holes, whose origin can be correlated to the target structure. Actually, if we consider the second SEM image (Fig. 4b), which is a photograph of a cross-section of the not yet ablated target, we can see a large number of structures that are probably structural defects or gas bubbles trapped into the solid during the glass formation. The cavities corresponding to the bubbles can be referred to the origin of the holes, while the explosive release of the gas contained in the bubbles can explain the large amount of droplets, coming from a melted phase, found on the substrate. These are other indications about a relatively low temperature on the target surface. As a matter of fact, the ejected particles should be cold enough to show no radiative emission at all in the UV–Vis range, as demonstrated from ICCD analysis.



(a)



(b)

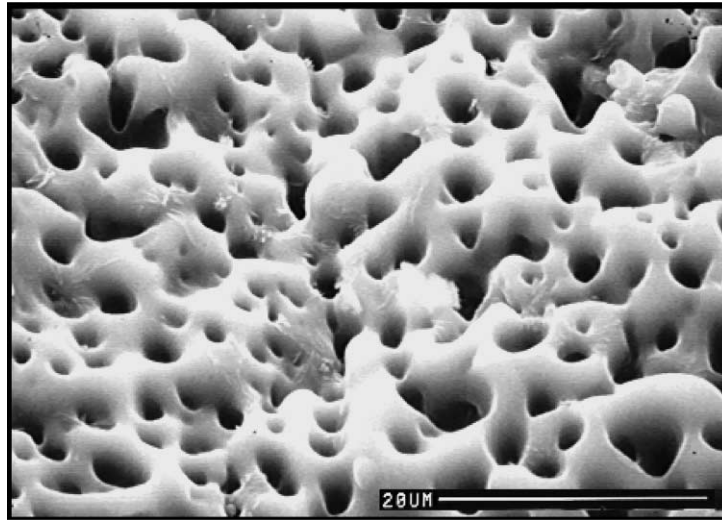
Fig. 3. SEM microphotographs: (a) surface of a Bioglass film deposited at a laser fluence of 7 J/cm^2 and (b) cross-section of the same film.

From an applicative point of view a useful Bioglass film should show the following characteristics: a good coverage degree of the substrate, good adhesion to the substrate and, mostly important, a bioactive behaviour.

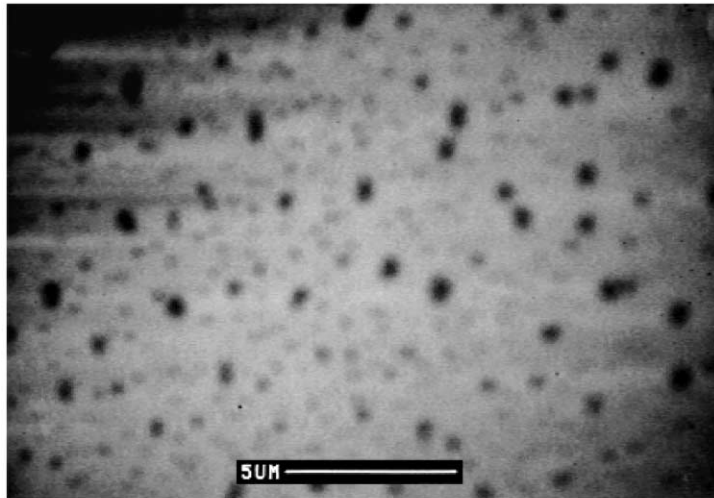
Fig. 5 shows the WDX single element distribution maps of a Bioglass film. The different colours refer to different concentration of the elements (from pink-great concentration, to grey-small concentration, to

black-total absence) but this is not a quantitative analysis. Our purpose is only to show that the substrate is completely covered by the film, as evidenced from the total absence of black spots in the first four images.

The adhesion measurements, performed by a scratch tester [14], show good results for all our films. In fact the mean pressure at the onset of the film deformation was 1.4 GPa while the substrate deformation



(a)



(b)

Fig. 4. SEM microphotographs: (a) ablated target surface and (b) cross-section of the not yet ablated target.

starts at 9.3 GPa. So it is easier to deformate the substrate than to detach the film [15].

To test the bioactivity of our films, we have dipped them into a simulating the body fluid solution (SBF) [16] and thermostated at 37°C, for different time scales. Afterwards, by X-ray diffraction, we have evaluated how the eventual growth of hydroxylapatite could be affected from the film SBF exposure time.

In Fig. 6, the X-ray diffraction spectra for a film left for 10 and 24 days in the SBF solution is reported. The main peaks belong to the substrate, but smaller peaks are characteristics of calcium hydroxylapatite. In particular, the 211 and 300 peaks are the most intense peaks in the reference hydroxylapatite spectrum [17], while the presence of an intense 002 peak indicates that in the first steps of hydroxylapatite growth the film is preferentially oriented [18].

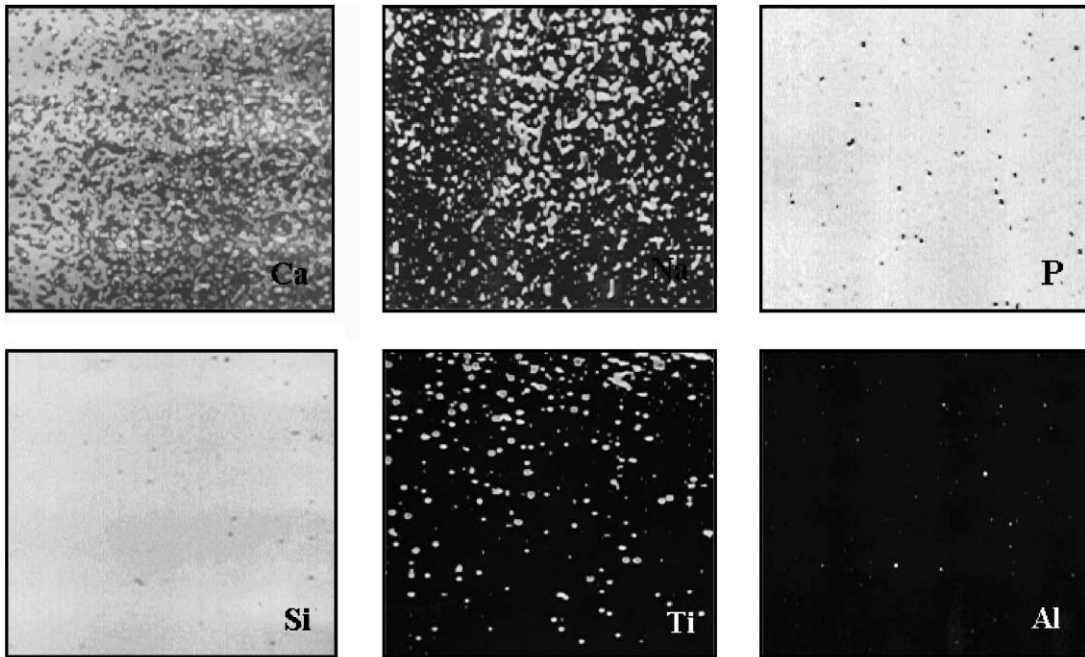


Fig. 5. WDX single element distribution maps of a Bioglass film.

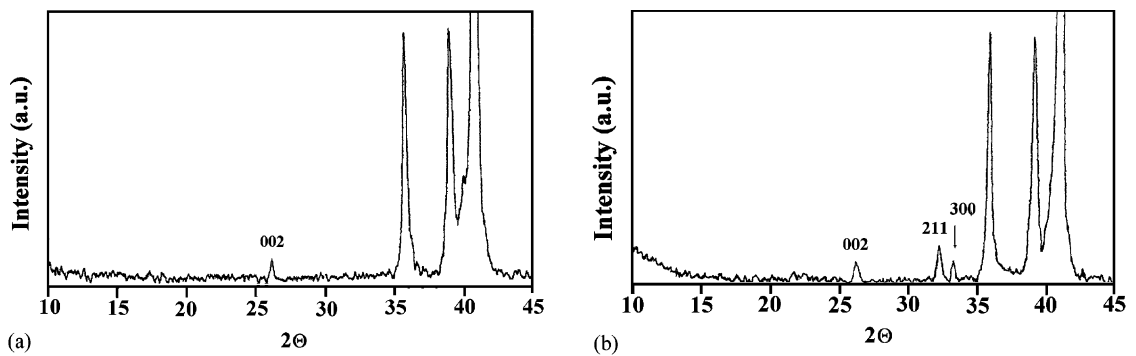


Fig. 6. X-ray diffraction spectra of a Bioglass film exposed to an SBF solution: (a) after 10 days and (b) after 24 days.

4. Conclusions

In conclusion, we have demonstrated that it is possible to obtain bioactive glass thin films by PLAD even if the vaporisation is far to be congruent. Our film is composed mainly of macroscopic particles directly emitted from the target and conserving the target stoichiometry. In this case the particulate, normally considered a drawback of the ablation–deposition process, plays a fundamental role in the Bioglass film formation. Once again, the versatility of PLAD technique has been confirmed. As future developments, since in our laboratory we have tested Bioglass films only in an SBF solution, we suggest to validate their bioactivity by both in vitro and in vivo assessments.

Acknowledgements

Special thanks are due to US Biomaterials for their supply of the Bioglass[®] 45S5 targets used in this work.

References

- [1] T. Kokubo in: P. Duran, J.F. Fernandez (Eds.), Proceedings of the Third Euro-Ceramics, Faenza Editrice Iberica, San Vicente, Vol. 3, 1993, p. 1.
- [2] J.D. Santos, P.L. Silva, J.C. Knowles, S. Talal, F.J. Monteiro, *J. Mater. Sci.: Mater. Med.* 7 (1996) 187.
- [3] P. Ducheyne, W. van Raemdonck, J.C. Heughebaert, M. Heughebaert, *Biomaterials* 7 (1986) 97.
- [4] S.D. Cook, J.F. Kay, K.A. Thomas, R.C. Anderson, J. Jarcho, *J. Dental Res.* 65 (1986) 222.
- [5] E. Ruckenstein, S. Gourisanker, R.E. Baier, *J. Coll. Interf. Sci.* 96 (1983) 245.
- [6] D.B. Chrisey, G.K. Hubler (Eds.), *Pulsed Laser Deposition of Thin Films*, Wiley, New York, 1994.
- [7] J.C. Miller, R.F. Haglund (Eds.), *Laser Ablation and Deposition, Experimental Methods in the Physical Science*, Vol. 30, Academic Press, London, 1998.
- [8] S.F. Hulbert, J.C. Bokros, L.L. Hench, J. Wilson, G. Heimke, in: P. Vincenzini (Ed.), *High Tech Ceramics*, Elsevier, Amsterdam, 1987, p. 3.
- [9] L. D'Alessio, R. Teghil, M. Zaccagnino, I. Zaccardo, D. Ferro, V. Marotta, *Appl. Surf. Sci.* 138–139 (1999) 527.
- [10] R.E. Russo, X. Mao, in: J.C. Miller, R.F. Haglund (Eds.), *Laser Ablation and Deposition, Experimental Methods in the Physical Science*, Vol. 30, Academic Press, London, 1998, p. 375.
- [11] A. Giardini Guidoni, A. Mele, T.M. Di Palma, C. Flamini, S. Orlando, R. Teghil, *Thin Solid Films* 295 (1997) 77.
- [12] W. Vogel, *Chemistry of Glass*, The American Chemical Society, Columbus, 1985.
- [13] R. Aveyard, J.H. Clint, D. Needs, *Eur. Microsc. Anal.* 29 (2000).
- [14] G. Czél, R. Teghil, D. Janovszky, R. Véghe, in: Proceedings of the International Conference on Competitive Materials, Technologies and Products CMTP, May 9–11, 2000, Miskolc, Hungary, p. 97.
- [15] C.M. Cotell, in: D.B. Chrisey, G.K. Hubler (Eds.), *Pulsed Laser Deposition of Thin Films*, Wiley, New York, 1994, p. 549.
- [16] T. Kokubo, H. Sushitani, S. Sakka, T. Kitsugi, T. Yamamuro, *J. Biomed. Mater. Res.* 24 (1990) 721.
- [17] P. Ducheyne, W. van Raemdonck, J.C. Heughebaert, M. Heughebaert, *Biomaterials* 7 (1986) 97.
- [18] I. Rehman, J.C. Knowles, W. Bonfield, *J. Biomed. Mater. Res.* 41 (1998) 162.